Environmental Science & Technology

Article

pubs.acs.org/est

Atmospheric Fate of Monoethanolamine: Enhancing New Particle Formation of Sulfuric Acid as an Important Removal Process

Hong-Bin Xie,*[,†,‡] Jonas Elm,[‡] Roope Halonen,[‡] Nanna Myllys,[‡] Theo Kurtén,[§] Markku Kulmala,[‡] and Hanna Vehkamäki[‡]

[†]Key Laboratory of Industrial Ecology and Environmental Engineering (Ministry of Education), School of Environmental Science and Technology, Dalian University of Technology, Dalian 116024, China

[‡]Department of Physics, University of Helsinki, P.O. Box 64, FIN-00014 Helsinki, Finland

[§]Department of Chemistry, University of Helsinki, P.O. Box 55, FIN-00014 Helsinki, Finland

Supporting Information

ABSTRACT: Monoethanolamine (MEA), a potential atmospheric pollutant from the capture unit of a leading CO_2 capture technology, could be removed by participating H_2SO_4-based new particle formation (NPF) as simple amines. Here we evaluated the enhancing potential of MEA on H_2SO_4-based NPF by examining the formation of molecular clusters of MEA and H_2SO_4 using combined quantum chemistry calculations and kinetics modeling. The results indicate that MEA at the parts per trillion (ppt) level can enhance H_2SO_4-based NPF. The enhancing potential of MEA is less than that of dimethylamine (DMA), one of the strongest enhancing agents, and much greater than methylamine (MA), in contrast to the order suggested solely by their basicity (MEA < MA < DMA). The unexpectedly high enhancing potential is attributed to the role of −OH of MEA in increasing cluster binding free energies by acting as both a hydrogen bond donor and acceptor. After the initial formation of one H_2SO_4 and one MEA cluster, the cluster growth mainly proceeds by first adding one H_2SO_4, and then one MEA, which differs from growth pathways in H_2SO_4−DMA and H_2SO_4−MA systems. Importantly, the effective removal rate of MEA due to participation in NPF is comparable to that of oxidation by hydroxyl radicals at 278.15 K, indicating NPF as an important sink for MEA.

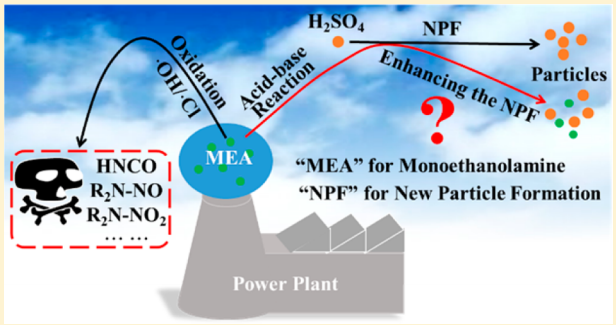

INTRODUCTION

Monoethanolamine (MEA, $NH_2CH_2CH_2OH$) is a benchmark and widely utilized solvent in amine-based postcombustion CO_2 capture (PCC) technology.[1−9] Given the possible large-scale implementation of amine-based PCC, it is likely that there will be relatively significant emissions of MEA or other alkanolamines to the atmosphere from PCC units due to their relatively high vapor pressure.[10] It has been estimated that a CO_2 capture plant which removes 1 million tons CO_2 per year from flue gas using MEA as a solvent could potentially emit 80 tons MEA into the atmosphere.[11,12] Therefore, in recent years concern about the atmospheric fate of the representative amine MEA has been increasing,[6,13−22] as MEA could potentially form an environmental risk.[11,12,17]

Several studies have addressed the removal of MEA by atmospheric oxidation.[6,13−22] The oxidation by hydroxyl radicals (·OH) has been considered to be its main degradation pathway, followed by chlorine radicals (·Cl) at daytime.[13] The nitrate radical may play a significant role in MEA oxidation at night, though very little is known about this pathway. The reaction rate constants of MEA with ·OH and ·Cl are on the order of 10^{-11} and 10^{-10} cm^3 $molecule^{-1}$ s^{-1}, respectively, translating to 2.6−3.6 h atmospheric lifetime.[6,13,14,18,19] More importantly, atmospheric oxidation of MEA by ·OH and ·Cl can produce potentially hazardous compounds (such as isocyanic acid, HNCO, nitramine, and nitrosamine),[6,13,19] which can increase the environmental risk of MEA emission. Besides oxidation, acid−base reaction could be another important sink for MEA. However, the atmospheric fate related to the basicity of MEA has received little attention until now.

Atmospheric aerosol particles, at least 50% of which originates from new particle formation (NPF), are known to affect human health and remain as one of the leading uncertainties in global climate modeling and prediction.[23−27] Many studies have shown that atmospheric bases such as ammonia and amines stabilize sulfuric acid clusters in the lower troposphere via acid−base reactions, and therefore enhance H_2SO_4-based NPF rates.[25,28−42] Compared to ammonia, amines, including monomethylamine (MA), dimethylamine

Received: May 3, 2017
Revised: June 18, 2017
Accepted: June 26, 2017
Published: June 26, 2017

DOI: 10.1021/acs.est.7b02294
Environ. Sci. Technol. 2017, 51, 8422−8431

(DMA), and trimethylamine (TMA), can bind much more strongly to sulfuric acid molecules[29,40−43] and thus can efficiently enhance clustering sulfuric acid.[43] Recent work by Almeida et al. performed at the CLOUD chamber at CERN shows that 5 ppt of dimethylamine can enhance NPF rates more than 10 000 times compared with the case of 5 ppt ammonia and is sufficient to produce particle formation rates of the same order of magnitude as observed in the atmosphere.[25] Besides ammonia, MA, DMA, and TMA, atmospheric diamines were recently found to efficiently enhance NPF.[44,45]

In a similar fashion to simple alkylamines, MEA can potentially influence NPF via acid−base reactions and therefore participating in NPF could be another atmospheric sink of MEA. A recent study highlighted the possible role of emitted amines from CO_2 capture unit of PCC in enhancing NPF.[25] The basicity of MEA is higher than that of ammonia and lower than that of methylamine and dimethylamine (pK_b values of MEA 4.50, MA 3.36, DMA 3.29, ammonia 5.70).[46] If judged solely by the basicity, MEA should have a higher enhancing effect on H_2SO_4-based NPF than NH_3, and lower effect than MA and DMA when atmospheric concentration of MEA is assumed to be similar to that of NH_3, MA, and DMA. From the point of molecular structure, MEA has additional −OH compared to ammonia, MA, and DMA. When forming clusters between MEA and H_2SO_4, the −OH group in MEA can form additional hydrogen bonds (H-bonds), which increase the binding energy of MEA with H_2SO_4. The conflicting effects of one favorable (more H-bonds) and one unfavorable factor (decreased basicity compared with methylamine and dimethylamine) could make it difficult to estimate how strong the enhancing effect of MEA will be. No previous studies have considered the potential role of alkanolamines in NPF involving H_2SO_4. An additional −OH in the amine may lead to a different NPF pathway and rate compared to the ammonia/MA/DMA−H_2SO_4 systems. Therefore, to obtain a complete view of the atmospheric fate of MEA and extend the current knowledge of NPF involving amines and H_2SO_4, information about the potential of MEA to participate in atmospheric NPF is crucial.

In this study, we investigate the initial step of atmospheric H_2SO_4-based NPF by examining the formation of molecular clusters of MEA and sulfuric acid using a combination of quantum chemistry calculations and kinetics modeling employing the Atmospheric Cluster Dynamics Code[47,48] (ACDC). Via systematic conformational searches, we have obtained minimum free energy structures of clusters of composition $(MEA)_m(SA)_n$ (m = 0−4 and n = 1−4, "SA" represents H_2SO_4). The corresponding thermodynamic data and previously reported results for pure sulfuric acid $(SA)_{1-4}$ clusters[49] are used in ACDC to obtain cluster formation pathways and kinetics in the MEA−H_2SO_4 system. In addition, the effect of hydration on the cluster formation kinetics of MEA and H_2SO_4 is considered.

COMPUTATIONAL DETAILS

Electronic Structure Calculations. The most critical parameters in identifying cluster formation pathways and kinetics are the cluster formation free energies. Both minimum free energy structures of clusters $(MEA)_m(SA)_n$ (m = 0−4 and n = 0−4) and computational method will determine the reliability of calculated cluster formation free energies. Here, a global minimum sampling technique (Figure 1), which has previously been applied to study atmospheric cluster

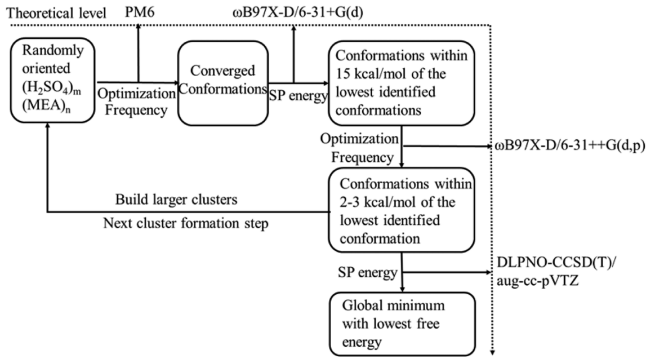

Figure 1. Flowchart for the multistep global minimum sampling method. "SP" represents a single point energy calculation.

formation,[45,50,51] was used to search for the global minima of clusters $(MEA)_m(SA)_n$ (m = 1−4 and n = 0−4). The pure $(SA)_{1-4}$ clusters were taken from the work of Ortega et al.[49] In Figure 1, all optimizations, frequency, or single point energy calculations with density functional theory and semiempirical PM6 level have been performed in GAUSSIAN 09.[52] The ωB97X-D functional was selected as the core optimization and frequency calculation method in Figure 1, since it has shown good performance for studying the formation of atmospheric molecular clusters.[53,54] Single point energy calculations at the DLPNO-CCSD(T) (domain-based local pair natural orbital coupled cluster[55,56])/aug-cc-pVTZ level have been performed in ORCA version 3.0.3.[57] Recent studies indicated that the DLPNO-CCSD(T) method can be used to calculate atmospheric acid−base clusters up to 10 molecules,[58] and the utilized DLPNO-CCSD(T)/aug-cc-pVTZ method has been shown to yield a mean absolute error of 0.3 kcal/mol compared to CCSD(T) complete basis set estimates, based on a test set of 11 small atmospheric cluster reactions.[54] The MEA monomer has 13 conformations,[6,59] and each was used as a starting point for forming the molecular clusters. For the global minimum search, more than 10 000 randomly oriented configurations were built for each cluster. We have estimated the Gibbs free energies for all obtained global minima at 298.15 K by combining the single point energies at the DLPNO-CCSD(T)/aug-cc-pVTZ level and Gibbs free energy correction terms at the ωB97X-D/6-31++G(d,p) level. The formation free energies for each cluster were obtained by subtracting Gibbs free energy of the constituent molecules from that of the cluster at 298.15 K. The formation free energies at other temperatures were calculated under the assumption that enthalpy and entropy change remain constant in the tropospheric temperature range.

To consider the effect of hydration, the $(MEA)_m(SA)_nW_x$ (m = 0−2, n = 0−2, x = 1−3, "W" represents H_2O) clusters were investigated. For their global minimum search, a similar scheme as for the clusters without water molecules was used. In addition, to directly compare the enhancing effect of MEA to ammonia, MA and DMA, we re-evaluated their formation free energies at the same theoretical level, based on reported cluster structures, or new lower energy structures (presented in Figure S1).[48,49,60] It should be noted that for global minimum of the unhydrated MA−SA clusters, only $(MA)_{0-3}(SA)_{0-3}$ is available,[41,60] and therefore, formation free energy data for MA are only for $(MA)_{0-3}(SA)_{0-3}$.

ACDC Model. We used ACDC to study the formation pathways, steady-state concentrations and formation rates of clusters. The detailed theory behind the ACDC was present in

DOI: 10.1021/acs.est.7b02294
Environ. Sci. Technol. 2017, 51, 8422−8431

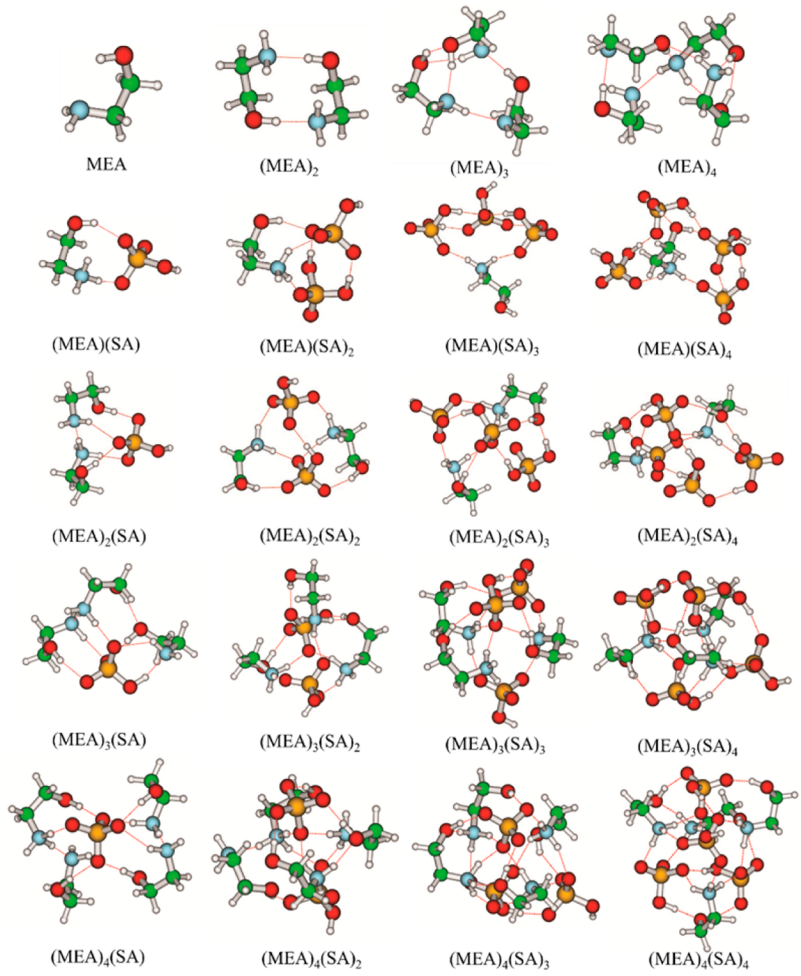

Figure 2. Structures of global free energy minima for $(MEA)_m(H_2SO_4)_n$ (m = 1−4 and n = 0−4) at the ωB97X-D/6-31++G(d,p) level of theory. The red balls represent oxygen atoms, blue is for nitrogen atoms, green is for carbon atoms, and white is for hydrogen atoms.

a study by McGrath et al.[47] Briefly, the code generates equations for the time derivatives of the concentrations of all studied clusters and uses the Matlab ode15s routine to solve differential equations and simulate the time-dependent cluster concentrations. The differential equations, also called birth−death equations, include source terms from collisions of smaller clusters and evaporations from larger clusters, and sink terms from collisions with other clusters and evaporations into smaller clusters. In addition, the cluster formation rate in ACDC is defined as the flux of clusters outside the system. Whether a cluster is allowed to be outside the system or not is judged by the boundary condition. The hydration effect was considered in ACDC by taking H_2O molecule as an environment to affect the collision or evaporation of base-acid cluster.[61] The simulated system is a "4 × 4 box" for unhydrated system, where 4 is the maximum number of H_2SO_4 or MEA molecules in the clusters. The $(MEA)_4(SA)_5$ and $(MEA)_5(SA)_5$ were allowed to grow out of the system and all other clusters crossing the box edge are brought back to the simulation box by monomer evaporations (see boundary condition in the Supporting Information (SI)). The ACDC simulations were primarily run at 278.15 K, with additional runs performed at 258.15, 268.15, 288.15, and 298.15 K to study the temperature effect. A constant coagulation sink coefficient of 2.6×10^{-3} s^{-1} was used as a sink term. This value corresponds to typical one observed in boreal forest environments.[48] The sulfuric acid concentration was set to be 10^5, 10^6, 10^7, 10^8, and 10^9 cm^{-3}, a range relevant to atmospheric NPF.[25,48,62] Atmospheric MEA concentrations were set to be 1, 10, and 100 ppt, a range relevant to atmospheric NPF for DMA.[25] It should be mentioned that the acid concentration $[H_2SO_4]$ was defined as the total concentration of all neutral clusters containing one acid and any number of base molecules, as in a previous study.[48] When hydration effect was considered, the simulated system is a "2 × 2 box". Average collision and evaporation coefficients over the hydrate distribution for each cluster of $(MEA)_m(SA)_n$ (m = 0−2, n = 0−2) were used in the birth−death equations for $[H_2SO_4] = 10^6$ and [MEA] = 10 ppt and at 278.15 K. The equilibrium hydrate distribution for each cluster was calculated by the equilibrium constant for the formation of the respective hydrate.[61] Similar to the definition of boundary condition of unhydrated MEA−SA cluster, $(MEA)_2(SA)_3$ and $(MEA)_3(SA)_3$ were allowed to grow out of the system. As a comparison, we also preformed ACDC simulation for MA−H_2SO_4 and DMA−H_2SO_4 systems at 278.15 K. The simulated system is a "3 × 3 box" for MA since only $(MA)_{0-3}(SA)_{0-3}$ is available, and a 4 × 4 box for DMA. The $(MA)_3(SA)_4$ and $(MA)_4(SA)_4$ and $(DMA)_4(SA)_5$ and $(DMA)_5(SA)_5$ were allowed to grow out of the simulation box for the MA−H_2SO_4 and DMA−H_2SO_4 systems (see the SI), respectively. Other ACDC simulation details are similar to those for MEA. In addition, ACDC simulation was performed

DOI: 10.1021/acs.est.7b02294
Environ. Sci. Technol. 2017, 51, 8422−8431

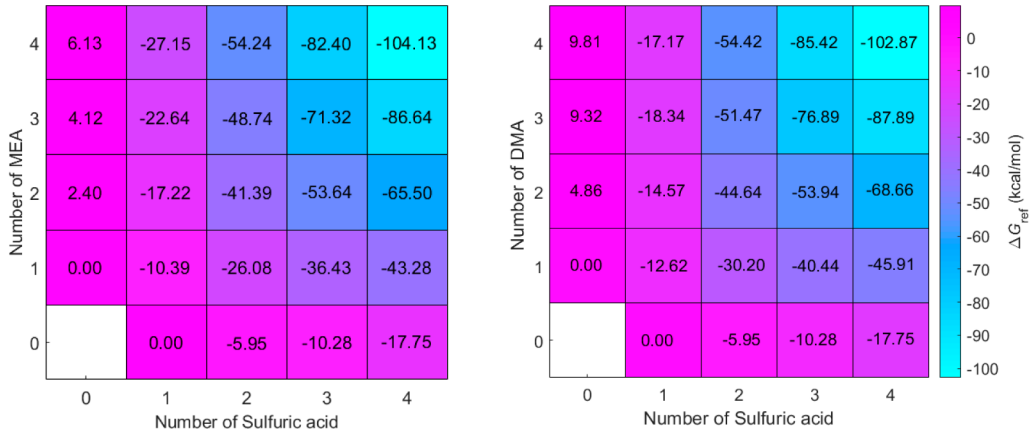

Figure 3. Calculated formation free energies for $(MEA)_m(SA)_n$ (left panel) and $(DMA)_m(SA)_n$ (right panel) clusters (m = 0−4 and n = 0−4) at the DLPNO-CCSD(T)/aug-cc-pVTZ//ωB97X-D/6-31++G(d,p) level and 298.15 K and 1 atm (reference pressure of acid and base).

for MEA−H_2SO_4 with a 3 × 3 box, to compare the MA−H_2SO_4 system with a similar simulation box size.

RESULTS AND DISCUSSION

Structures and Thermodynamic Data. We use $(MEA)_m(SA)_n$ to represent the cluster formed by m MEA molecules and n H_2SO_4 molecules to avoid explicitly specifying the proton transfer status. Since previous studies have discussed the structures of pure H_2SO_4 clusters,[49] here, we mainly focus on the clusters $(MEA)_m(SA)_n$ (m = 1−4 and n = 0−4). The structures of $(MEA)_m(SA)_n$ are shown in Figure 2. Generally, in the homomolecular clusters $(MEA)_m$, no proton transfer has occurred and clusters are stabilized mainly by H-bonds. In all heteromolecular clusters, proton transfer is observed, and clusters are stabilized by both H-bonds and electrostatic interaction between positive and negative species. When $n \geq m$, the amine ($-NH_2$) groups of all MEA molecules are protonated by H_2SO_4. In this case H_2SO_4 only transfers a single proton and in no cases a sulfate ion is formed. When $n < m$, there are two different proton transfer pattern. For $(MEA)_2(SA)$ and $(MEA)_3(SA)$ clusters, one proton of H_2SO_4 is donated, and therefore, not all MEA molecules are protonated. For $(MEA)_4(SA)$, $(MEA)_4(SA)_2$, $(MEA)_4(SA)_3$, and $(MEA)_3(SA)_2$, H_2SO_4 can donate two protons, and therefore, all MEAs are protonated in the case of $m - n = 1$ ($(MEA)_4(SA)_3$ and $(MEA)_3(SA)_2$), while MEA is not completely protonated in the case of $m - n > 1$ ($(MEA)_4(SA)$ and $(MEA)_4(SA)_2$). The above proton transfer patterns for H_2SO_4−MEA clusters are similar to those of H_2SO_4−DMA clusters.[48,49]

Another structural feature in all clusters except $(MEA)(SA)_3$ is that −OH groups of all MEAs can form at least one H-bond with H_2SO_4 as H-bond donors. In many cases such as $(MEA)_3$, $(MEA)_4$, $(MEA)(SA)_4$, $(MEA)_2(SA)_3$, $(MEA)_2(SA)_4$, $(MEA)_3(SA)_1$, $(MEA)_3(SA)_2$, $(MEA)_3(SA)_4$, $(MEA)_3(SA)_2$, $(MEA)_4(SA)_2$, and $(MEA)_4(SA)_3$ clusters, the −OH group of MEA can form another H-bond with the −OH group of H_2SO_4, ammonium cation ($-RNH_3^+$) of protonated MEA or −OH of MEA as an H-bond acceptor. The involvement of the −OH group of MEA leads to a preference for a spherical three-dimensional structure, especially for the studied large cluster sizes. As an exception, for $(MEA)(SA)_3$, we also located a low-energy minimum (Figure S2) involving H-bonds where −OH group of MEA acts as both a hydrogen bond donor and acceptor. However, the configuration is not the global minimum for the Gibbs free energy. The binding energy of this minimum is about 1 kcal/mol lower than that of the free energy global minimum shown in Figure 2 and, thus, unfavorable entropy effects are taking place in this configuration.

It is known that DMA is one of the strongest agents for enhancing atmospheric H_2SO_4-based NPF.[25,29,43] Here, we take formation free energies of the H_2SO_4−DMA system as a reference to discuss the formation free energies of H_2SO_4−MEA. The free energy data at 298.15 K for the formation of the clusters from their constituent molecules for the MEA/DMA−H_2SO_4 system are presented in Figure 3, and the corresponding thermodynamical quantities ΔH and ΔS are presented in Table S1. For the pure base clusters, formation free energy of all MEA clusters is lower than that of corresponding DMA clusters. This results from the fact that there is one more H-bond bonding agent (−OH) in MEA compared with DMA, which leads to more H-bonds in the pure MEA clusters than that in the corresponding DMA clusters. The formation free energy for most heteromolecular H_2SO_4−MEA clusters is 0.2−5.6 kcal/mol higher than that of corresponding H_2SO_4−DMA clusters. However, the formation free energies for $(MEA)_2SA$, $(MEA)_3SA$, $(MEA)_4SA$, and $(MEA)_4(SA)_4$ are lower than those of the corresponding clusters from DMA. The difference in formation free energies of MEA clusters, compared with DMA clusters, originates from the competition between the unfavorable (lower basicity of MEA than that of DMA) and favorable factor (the formation of more H-bonds from the −OH group of MEA) for forming clusters. In addition, we noted that formation free energies of MEA−H_2SO_4 clusters are lower than those of the corresponding MA−H_2SO_4 clusters (Figure S3) although basicity of MEA is much lower than that of MA, indicating that the −OH group in MEA does indeed play an important role in the cluster formation between MEA and H_2SO_4. In a recent study, Chen et al. revealed that besides the basicity, the hydrogen-bonding capacity of the $-NH_x$ (x = 1−3) group in amine/ammonia can play an important role in enhancing methanesulfonic acid driven NPF.[63] Our findings and Chen et al.'s study[63] together show the importance of molecular interactions involving the $-NH_x$ (x = 1−3) group and other functional groups of amines in NPF. In addition, similar to MA and DMA, the formation free energies for MEA are much lower than those of NH_3 (Figure S3) with H_2SO_4.

DOI: 10.1021/acs.est.7b02294
Environ. Sci. Technol. 2017, 51, 8422−8431

Evaporation Rates. In view of the acid−base cluster growth, the stability of the cluster can be deduced by comparing the evaporation rate with the collision rate, which mainly depends on the collision rate constant and the concentration of the acid and base molecules. However, the collision rate constants for the studied clusters are very close to each other and thus difference in the evaporation rate can be used to represent the stability of clusters at the given acid and base concentration. The evaporation rates for $(MEA)_m(SA)_n$ on the MEA−SA grid at 278.15 K are presented in Figure 4.

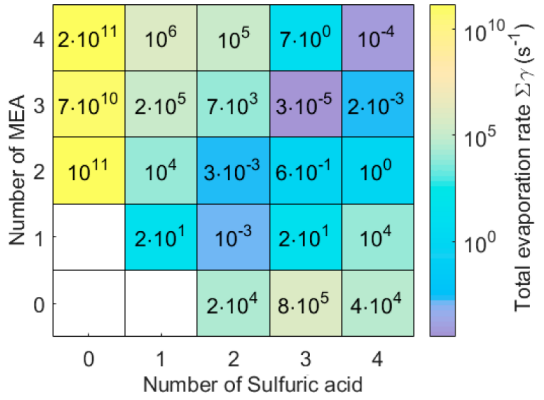

Figure 4. Evaporation rates for $(MEA)_m(SA)_n$ on the MEA−SA grid at 278.15 K.

Generally, evaporation rates for clusters $(MEA)_2(SA)_2$, $(MEA)_1(SA)_2$, $(MEA)_3(SA)_3$, $(MEA)_3(SA)_4$, and $(MEA)_4(SA)_4$ are of the order of 10^{-3}−10^{-5} s^{-1}, which is much lower than those for other studied cluster sizes. When the concentration of MEA or H_2SO_4 is around or above ppt level, those clusters with evaporation rate 10^{-3}−10^{-5} s^{-1} can be considered to be stable, and $(MEA)_3(SA)_3$ and $(MEA)_4(SA)_4$ are the most stable clusters (see discussion on stability of clusters in the SI). By checking all evaporation pathways (see Table S2), evaporation of a H_2SO_4 or MEA monomer is found to be the main decay route for all clusters studied here. If m and n are unequal, evaporation of species with a greater number of molecules is always preferred. For clusters with $m = n > 2$, evaporation of MEA is faster than that of H_2SO_4. In addition, when there is equal number of molecules in two clusters, the evaporation rate of MEA abundant cluster is higher than corresponding H_2SO_4 abundant cluster, indicating that the bonding ability of H_2SO_4 to the cluster is stronger than that of MEA. A similar phenomena concerning the stronger bonding ability of acid is also found in other acid−base cluster systems, such as DMA-SA, NH_3−H_2SO_4, and NH_3−HNO_3.[49,64]

It is also interesting to compare cluster evaporate rates for the different amines (MA, DMA, and MEA) at the same simulation condition. For most of the clusters, including heteromolecular and pure base clusters, the evaporation rates for MEA clusters are lower than corresponding ones for MA and DMA (Figure S4) clusters. However, it is not straightforward to conclude which amine can form the most stable clusters as evaporation rates for a couple of clusters with MA and DMA are lower than those of MEA clusters. If the initially formed one SA and one base cluster (which are crucial for cluster growth at relevant H_2SO_4 and base concentration for MEA, MA and DMA as discussed in the Growth Pathways section) are compared, evaporate rate of (MEA)(SA) is lower than that of (MA)(SA) and higher than that of (DMA)(SA). Therefore, the stability of initially formed clusters for the three types of amine−H_2SO_4 clusters follows the trend (DMA)(SA) > (MEA)(SA) > (MA)(SA) at the given acid and base concentrations. In addition, in accordance with a previous study,[47] the evaporation of small clusters is found to be the main decay route for some of DMA−H_2SO_4 clusters. This is not the case for MEA−SA and MA−SA clusters, where monomer evaporation is dominant. This results from the higher stability of the small DMA−H_2SO_4 clusters.

Steady-State Cluster Concentrations and Formation Rates. The steady-state sulfuric acid dimer concentration (all clusters including sulfuric acid dimer) and the formation rate of clusters growing out of the simulation box can be taken as two important quantities characterizing the stabilization potential of a given base in H_2SO_4-based NPF.[25,43,60] Figure 5 shows the steady-state sulfuric acid dimer concentration and the cluster formation rate as a function of monomer concentration (H_2SO_4 concentration in the range 10^5−10^9 cm^{-3}, MEA mixing ratios of 1−100 ppt) at 278.15 K for MEA−H_2SO_4 clusters, along with DMA−H_2SO_4 and MA−H_2SO_4 clusters as a comparison. Generally, the sulfuric acid dimer concentration and the cluster formation rate increase with increasing the concentrations of MEA and H_2SO_4 at the considered condition. The MEA concentration dependence of the sulfuric acid dimer concentration and the cluster formation rate weakens with increasing H_2SO_4 concentration, indicating that the system gradually approaches saturation with respect to MEA at a high H_2SO_4 concentration. Similar behavior is also found in the simulations with MA and DMA as base. More importantly, MEA yields roughly 10−10^2-fold dimer concentration and 10^2−10^3-fold formation rate compared to the simulations with MA as a base,

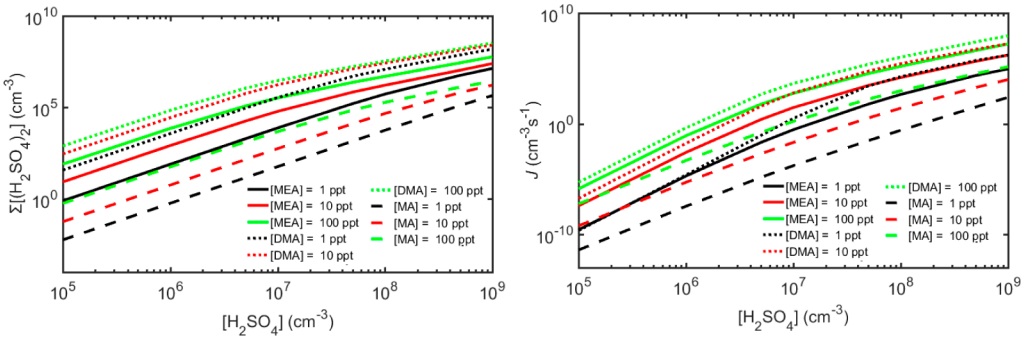

Figure 5. Simulated steady-state H_2SO_4 dimer concentration $\sum[(H_2SO_4)_2]$ (cm^{-3}) (left panel) and the cluster formation rate J (cm^{-3} s^{-1}) out of the simulation system (right panel) as a function of monomer concentration at 278.15 K.

DOI: 10.1021/acs.est.7b02294
Environ. Sci. Technol. 2017, 51, 8422−8431

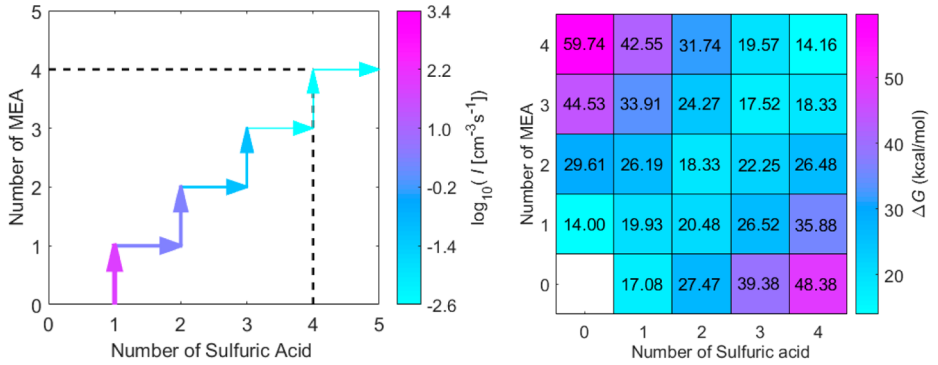

Figure 6. Main clustering pathways (left panel) and actual Gibbs free energy surface for the formation of clusters $MEA_m(H_2SO_4)_n$ (right panel) at 278.15 K, $[H_2SO_4] = 10^6$ cm^{-3}, and [MEA] = 10 ppt. For figure clarity, the pathways contributing less than 5% to the flux of the cluster are not shown.

and 0.02−0.2-fold dimer concentration and 0.02−1-fold formation rate as compared to the simulations with DMA as a base, indicating the order of the stabilization potential of these three amines follows: DMA > MEA > MA. It deserves mentioning that MEA−H_2SO_4 formation rates compared to MA−H_2SO_4 become even higher if the same simulation box size is used for MEA and MA (3 × 3) (formation rate of MEA−H_2SO_4 will increase 1.1−6 times, compared with a 4 × 4 box). However, the difference in sulfuric acid dimer concentration was similar to different simulation box sizes. As experimental evidence has shown that DMA and MA have an enhancing effect on H_2SO_4-based NPF at the parts per trillion (ppt) level,[25,43] it can be expected that MEA will have a similar effect with magnitude in between DMA and MA. Therefore, we can conclude that MEA can enhance NPF of H_2SO_4 when the atmospheric concentration of MEA reaches ppt level. The higher stabilization potential of MEA, compared with MA, further verifies the important role of the −OH group of MEA in enhancing NPF involving H_2SO_4, as the basicity of MEA is lower than that of MA. In addition, both the sulfuric acid dimer concentration and the formation rate present negative temperature dependence in the range of 260−300 K, relevant to tropospheric conditions as shown in Figure S5. The negative temperature dependence effect is more prominent at lower MEA (1 ppt) and lower H_2SO_4 concentrations (10^6 cm^{-3}).

Growth Pathways. Figure 6 presents the growth pathway and the actual Gibbs free energy surface[47] for MEA and H_2SO_4 clusters at $[H_2SO_4] = 10^6$ cm^{-3}, [MEA] = 10 ppt, and 278.15 K. The actual Gibbs free energy surface was obtained by converting the change of free energy from 1 atm to the actual vapor pressures of the components.[47] As can be seen in Figure 6 (left panel), the first step in the growth is the binding of one H_2SO_4 molecule to a MEA molecule. After the initial step, the growth mainly proceeds by first adding one H_2SO_4, and then one MEA. The main flux out of the system is the $(MEA)_4(SA)_5$ cluster. Combining the growth pathway with the actual Gibbs free energy surface (right panel in Figure 6), two features can be observed. First, clusters do not follow the lowest free energy pathways ($(MEA)_1(SA)_1 \rightarrow (MEA)_2(SA)_2 \rightarrow (MEA)_3(SA)_3 \rightarrow (MEA)_4(SA)_4$), which would involve the cluster collision with $(MEA)_1(SA)_1$ cluster. This results from fact that the concentration of the $(MEA)_1(SA)_1$ cluster (5.73×10^3 cm^{-3}) is much lower than that of the H_2SO_4 monomer (9.94×10^5 cm^{-3}). Second, the addition of H_2SO_4 monomers involves a small free energy barrier, but the addition of MEA does not. Furthermore, combining the growth pathway with the evaporation rate of the clusters, we can conclude that the formation of initial cluster $(MEA)_1(SA)_1$ is the rate-determining step for the cluster growth since the $(MEA)_1(SA)_1$ cluster is much more unstable than other clusters in the cluster growth pathway and readily evaporates back into MEA and SA monomers.

We also compared the growth pathways for MEA−H_2SO_4 with MA−H_2SO_4 and DMA−H_2SO_4 system at the same simulation conditions. The formation pathways for MA−H_2SO_4 and DMA−H_2SO_4 are presented in Figure S6. A common feature is that the initially formed cluster mainly consists of one H_2SO_4 and one base molecule for all three amines. However, as a whole, the growth pathway for the MEA−H_2SO_4 system is significantly different from that of the MA−H_2SO_4 and DMA−H_2SO_4 systems. In accordance with a previous study,[47] collisions involving the $(DMA)_1(SA)_1$ cluster contribute significantly to the growth for DMA−SA system, which makes the growth occur mainly along the diagonal on the acid−base grid. In contrast to MEA and DMA, the cluster growth for the MA system does not follow the diagonal direction and the formation of larger clusters $(MA)_1(SA)_2$ and $(MA)_2(SA)_3$ has two pathways either via addition of H_2SO_4 or MA. The sulfuric acid dimer has a significant population in the initial clusters, which results from the low stability of the $(MA)_1(SA)_1$ cluster.

Effect of Hydration. As water is many orders of magnitude more abundant than sulfuric acid and bases in the atmosphere, hydration might change the cluster formation free energies and therefore cluster formation kinetics[61,65,66] Previous studies have found that clusters consisting of H_2SO_4 and DMA or ammonia are mainly hydrated by less than three H_2O molecules.[30,61] We expected that MEA−H_2SO_4 clusters could still be hydrated by less than three H_2O molecules although the structure of MEA is different from DMA and ammonia. Here, 1−3 H_2O molecules were considered to study the effect of hydration on the formation kinetics of MEA−H_2SO_4 clusters. In addition, to save computational resources, we only selected the smallest clusters $(MEA)_m(SA)_n$ (m = 0−2, n = 0−2) as test system to investigate the hydration. Based on the calculated equilibrium hydrate distribution of the clusters at relative humidities (RH) 20%, 50%, and 100%, at 278.15 K, converted from calculated Gibbs free energies of stepwise hydration at 278.15 K and 1 atm, we can conclude that sulfuric acid−MEA clusters are only mildly hydrated (0−2 H_2O molecules depending on RH). Details for the discussion on calculated Gibbs free energies of stepwise hydration, optimized structures and the hydrate distribution of

DOI: 10.1021/acs.est.7b02294
Environ. Sci. Technol. 2017, 51, 8422−8431

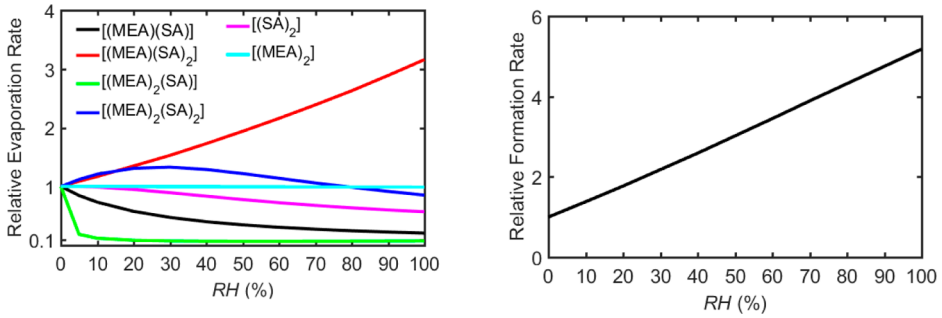

Figure 7. Relative evaporation rate (left panel) and cluster formation rate ($[H_2SO_4] = 10^6$ cm^{-3} and [MEA] = 10 ppt) (right panel) as a function of relative humidity at 278.15 K.

the clusters are presented in the SI. Here, we mainly focus on the effect of hydration on the cluster formation kinetics.

In principle, hydration can affect the cluster formation rate both through the collision and evaporation rates. However, hydration was found to have little effect on the collision rate since the collision diameter, an important factor in collision rate coefficients in kinetic collision theory employed in ACDC, changes very little with hydration.[61] Hence, only the effect of hydration on the evaporation rates and formation rates will be discussed in detail. Figure 7 presents the evaporation rates (left) and formation rates (right) as a function of RH at 278.15 K compared to dry conditions. Clearly, the presence of water has various effects on the evaporation rate depending on the given cluster. Water has a little effect on the evaporation rate of the $(SA)_2$ and $(MEA)_2(SA)_2$ and almost no effect on that of the $(MEA)_2$ cluster. However, the evaporation rate of $(MEA)(SA)_2$ can be increased up to 3 times by hydration and that of $(MEA)_2(SA)$ can be decreased by 13 times compared to the dry case. More importantly, the presence of water decreases the evaporation rate of initially formed (MEA)(SA) clusters, i.e. the rate-determining step for cluster growth in the system, and this trend gradually increases with RH, which explains the increased cluster formation rate with increasing RH (right panel in Figure 7).The formation rate can be increased about 5-fold at RH = 100% compared to the dry case. It should be mentioned that although the absolute formation rate obtained from a small simulation box (2 × 2) is not reliable, the relative formation rate presented here should cancel out any significant bias introduced by the small simulation box. Generally, from these small cluster hydration simulations, we can conclude that hydration can slightly influence the evaporation rate, but the effect is in all cases relatively low and does not severely influence the results. Although it is not expected that qualitative conclusion from current study could be changed when larger clusters and more water molecules are used, future study with larger clusters and more water molecules is still deserved, to reach a more definitive conclusion about the RH effect on MEA−H_2SO_4 cluster formation kinetics.

Atmospheric Implications. We found that MEA at the ppt level can enhance the H_2SO_4-based NPF. The enhancing potential of MEA for NPF is lower than that of DMA, which is one of the strongest agents for enhancing H_2SO_4-based NPF,[25,43] and much higher than that of MA. In addition, we have shown that the −OH group of MEA plays an important role in enhancing H_2SO_4-based NPF due to the formation of additional H-bonds with H_2SO_4. To the best of our knowledge, this is the first study to point out the significant effect of one additional functional group in amines and show that the basicity of bases is not necessarily the only determining factor influencing H_2SO_4 driven NPF. Besides anthropogenic emission,[67] the oxidation of aliphatic amines could introduce −OH or keto-, peroxy-, and carboxylic acid groups in the atmosphere.[31,68,69] Amines including these additional H-bond donor/acceptor functional groups can enhance the NPF via a synergetic role of the basicity and the formation of additional H-bonds, especially for strongly basic amines. As the enhancing effect is very dependent on the exact structure of the molecule, the effect of these amines on NPF deserves further investigation.

Obviously, the participation of MEA in H_2SO_4-based NPF is a sink of the emitted MEA. It is known that the reaction with ·OH is an important sink for MEA due to a high reaction rate constant (k_{OH} 8.1×10^{-11} cm^3 molecule^{-1} s^{-1} at 278.15 K) and concentration of ·OH (9.7×10^5 cm^{-3}).[18] During the daytime, H_2SO_4 and ·OH can coexist in the atmosphere and the atmospheric concentration of H_2SO_4 (1×10^6 −1.9×10^7 cm^{-3} depending on the location)[70−72] is usually 1−19 times that of ·OH. We estimated the relative contribution of H_2SO_4 to ·OH for the removal of MEA by $k_{H2SO4}[H_2SO_4]/k_{OH}[\cdot OH]$ at 278.15 K, where k_{H2SO4} is removal rate constants of MEA for the participation in NPF involving H_2SO_4 and its value is estimated to be 2.16×10^{-11} and 5.6×10^{-11} cm^3 molecule^{-1} s^{-1} at dry or 50% RH condition, respectively (computational details in the SI). The contribution of H_2SO_4 to the removal of MEA is calculated to be about 0.27−5.2 and 0.7−13.1 times that of ·OH at dry and 50% RH conditions, respectively. This means that reactions with H_2SO_4 will compete with oxidation by ·OH in the atmosphere for the removal of MEA at tropospheric condition. Especially in regions where the concentration of H_2SO_4 is high, NPF might be the dominant removal process of gas-phase MEA. Therefore, the participation of MEA in H_2SO_4-based NPF should be considered when assessing the environmental risk of MEA emissions related to, for example, postcombustion CO_2 capture technology.

■ ASSOCIATED CONTENT

Supporting Information

The Supporting Information is available free of charge on the ACS Publications website at DOI: 10.1021/acs.est.7b02294.

Details for boundary conditions, discussion on the stability of clusters, hydration free energies, removal rate constants of MEA in NPF of H_2SO_4, thermochemical information for the formation of molecular clusters, evaporation coefficients for all evaporation pathways of different clusters, lower energy structures for NH_3−H_2SO_4 and dimethylamine (DMA)−H_2SO_4, low energy structure involving the hydrogen bonds between −OH of

DOI: 10.1021/acs.est.7b02294
Environ. Sci. Technol. 2017, 51, 8422−8431

all MEA and H_2SO_4, Formation free energies for the clusters for MA/NH_3−H_2SO_4, evaporation rates for MA/DMA−H_2SO_4 clusters, the cluster formation rates and steady-state H_2SO_4 dimer concentrations as a function of temperature, the main clustering pathways for MA/DMA−H_2SO_4 clusters, hydrate distribution of clusters and coordinates of all optimized clusters (PDF)

AUTHOR INFORMATION

Corresponding Author

*Phone/fax: +86-411-84707844. E-mail: hbxie@dlut.edu.cn.

ORCID

Jonas Elm: 0000-0003-3736-4329

Theo Kurtén: 0000-0002-6416-4931

Notes

The authors declare no competing financial interest.

ACKNOWLEDGMENTS

We thank the National Natural Science Foundation of China (21677028, 21325729) and ERC 692891-DAMOCLES. We thank the CSC-IT Center for Science in Espoo, Finland, for computational resources, J.E. thanks the Carlsberg Foundation for financial support, and H.-B.X. thanks the China Scholarship Council.

REFERENCES

(1) Veawab, A.; Tontiwachwuthikul, P.; Chakma, A. Corrosion Behavior of Carbon Steel in the CO_2 Absorption Process Using Aqueous Amine Solutions. *Ind. Eng. Chem. Res.* **1999**, *38* (10), 3917−3924.

(2) Liu, Y.; Zhang, L.; Watanasiri, S. Representing Vapor−Liquid Equilibrium for an Aqueous MEA-CO_2 System Using the Electrolyte Nonrandom-Two-Liquid Model. *Ind. Eng. Chem. Res.* **1999**, *38* (5), 2080−2090.

(3) Puxty, G.; Rowland, R.; Allport, A.; Yang, Q.; Bown, M.; Burns, R.; Maeder, M.; Attalla, M. Carbon Dioxide Postcombustion Capture: A Novel Screening Study of the Carbon Dioxide Absorption Performance of 76 Amines. *Environ. Sci. Technol.* **2009**, *43* (16), 6427−6433.

(4) Xie, H.-B.; He, N.; Song, Z.; Chen, J.; Li, X. Theoretical Investigation on the Different Reaction Mechanisms of Aqueous 2-Amino-2-methyl-1-propanol and Monoethanolamine with CO_2. *Ind. Eng. Chem. Res.* **2014**, *53* (8), 3363−3372.

(5) Xie, H.-B.; Johnson, J. K.; Perry, R. J.; Genovese, S.; Wood, B. R. A Computational Study of the Heats of Reaction of Substituted Monoethanolamine with CO_2. *J. Phys. Chem. A* **2011**, *115* (3), 342−350.

(6) Xie, H.-B.; Li, C.; He, N.; Wang, C.; Zhang, S.; Chen, J. Atmospheric Chemical Reactions of Monoethanolamine Initiated by OH Radical: Mechanistic and Kinetic Study. *Environ. Sci. Technol.* **2014**, *48* (3), 1700−1706.

(7) Xie, H.-B.; Wei, X.; Wang, P.; He, N.; Chen, J. CO_2 Absorption in an Alcoholic Solution of Heavily Hindered Alkanolamine: The Reaction Mechanism of 2-(tert-butylamino)- ethanol with CO_2 Revisited. *J. Phys. Chem. A* **2015**, *119*, 6346−6353.

(8) Xie, H.-B.; Zhou, Y.; Zhang, Y.; Johnson, J. K. Reaction Mechanism of Monoethanolamine with CO_2 in Aqueous Solution from Molecular Modeling. *J. Phys. Chem. A* **2010**, *114* (43), 11844−11852.

(9) da Silva, E. F.; Booth, A. M. Emissions from Postcombustion CO_2 Capture Plants. *Environ. Sci. Technol.* **2013**, *47* (2), 659−660.

(10) Kapteina, S.; Slowik, K.; Verevkin, S. P.; Heintz, A. Vapor Pressures and Vaporization Enthalpies of a Series of Ethanolamines. *J. Chem. Eng. Data* **2005**, *50* (2), 398−402.

(11) Karl, M.; Wright, R. F.; Berglen, T. F.; Denby, B. Worst Case Scenario Study to Assess the Environmental Impact of Amine Emissions from a CO_2 Capture Plant. *Int. J. Greenhouse Gas Control* **2011**, *5* (3), 439−447.

(12) Veltman, K.; Singh, B.; Hertwich, E. G. Human and Environmental Impact Assessment of Postcombustion CO_2 Capture Focusing on Emissions from Amine-Based Scrubbing Solvents to Air. *Environ. Sci. Technol.* **2010**, *44* (4), 1496−1502.

(13) Xie, H.-B.; Ma, F.; Wang, Y.; He, N.; Yu, Q.; Chen, J. Quantum Chemical Study on ·Cl-Initiated Atmospheric Degradation of Monoethanolamine. *Environ. Sci. Technol.* **2015**, *49* (22), 13246−13255.

(14) Karl, M.; Dye, C.; Schmidbauer, N.; Wisthaler, A.; Mikoviny, T.; D'Anna, B.; Müller, M.; Borrás, E.; Clemente, E.; Muñoz, A.; Porras, R.; Ródenas, M.; Vázquez, M.; Brauers, T. Study of OH-initiated Degradation of 2-aminoethanol. *Atmos. Chem. Phys.* **2012**, *12* (4), 1881−1901.

(15) Karl, M.; Svendby, T.; Walker, S. E.; Velken, A. S.; Castell, N.; Solberg, S. Modelling atmospheric oxidation of 2-aminoethanol (MEA) emitted from post-combustion capture using WRF−Chem. *Sci. Total Environ.* **2015**, *527*−*528*, 185−202.

(16) Nielsen, C. J.; D'Anna, B.; Dye, C.; Graus, M.; Karl, M.; King, S.; Maguto, M. M.; Müller, M.; Schmidbauer, N.; Stenstrøm, Y.; Wisthaler, A.; Pedersen, S. Atmospheric chemistry of 2-aminoethanol (MEA). *Energy Procedia* **2011**, *4*, 2245−2252.

(17) Nielsen, C. J.; Herrmann, H.; Weller, C. Atmospheric Chemistry and Environmental Impact of the Use of Amines in Carbon Capture and Storage (CCS). *Chem. Soc. Rev.* **2012**, *41* (19), 6684−6704.

(18) Onel, L.; Blitz, M. A.; Seakins, P. W. Direct Determination of the Rate Coefficient for the Reaction of OH Radicals with Monoethanol Amine (MEA) from 296 to 510 K. *J. Phys. Chem. Lett.* **2012**, *3* (7), 853−856.

(19) Borduas, N.; Abbatt, J. P. D.; Murphy, J. G. Gas Phase Oxidation of Monoethanolamine (MEA) with OH Radical and Ozone: Kinetics, Products, and Particles. *Environ. Sci. Technol.* **2013**, *47* (12), 6377−6383.

(20) da Silva, G. Atmospheric Chemistry of 2-Aminoethanol (MEA): Reaction of the NH_2•$CHCH_2OH$ Radical with O_2. *J. Phys. Chem. A* **2012**, *116* (45), 10980−10986.

(21) Manzoor, S.; Simperler, A.; Korre, A.; Theoretical, A. Study of the Reaction Kinetics of Amines Released into the Atmosphere from CO_2 Capture. *Int. J. Greenhouse Gas Control* **2015**, *41*, 219−228.

(22) Onel, L.; Blitz, M. A.; Breen, J.; Rickard, A. R.; Seakins, P. W. Branching Ratios for the Reactions of OH with Ethanol Amines Used in Carbon Capture and the Potential Impact on Carcinogen Formation in the Emission Plume from a Carbon Capture Plant. *Phys. Chem. Chem. Phys.* **2015**, *17* (38), 25342−25353.

(23) Zhang, R.; Suh, I.; Zhao, J.; Zhang, D.; Fortner, E. C.; Tie, X.; Molina, L. T.; Molina, M. J. Atmospheric New Particle Formation Enhanced by Organic Acids. *Science* **2004**, *304* (5676), 1487−1490.

(24) Winkler, P. M.; Steiner, G.; Vrtala, A.; Vehkamäki, H.; Noppel, M.; Lehtinen, K. E. J.; Reischl, G. P.; Wagner, P. E.; Kulmala, M. Heterogeneous Nucleation Experiments Bridging the Scale from Molecular Ion Clusters to Nanoparticles. *Science* **2008**, *319* (5868), 1374−1377.

(25) Almeida, J.; Schobesberger, S.; Kurten, A.; Ortega, I. K.; Kupiainen-Maatta, O.; Praplan, A. P.; Adamov, A.; Amorim, A.; Bianchi, F.; Breitenlechner, M.; David, A.; Dommen, J.; Donahue, N. M.; Downard, A.; Dunne, E.; Duplissy, J.; Ehrhart, S.; Flagan, R. C.; Franchin, A.; Guida, R.; Hakala, J.; Hansel, A.; Heinritzi, M.; Henschel, H.; Jokinen, T.; Junninen, H.; Kajos, M.; Kangasluoma, J.; Keskinen, H.; Kupc, A.; Kurten, T.; Kvashin, A. N.; Laaksonen, A.; Lehtipalo, K.; Leiminger, M.; Leppa, J.; Loukonen, V.; Makhmutov, V.; Mathot, S.; McGrath, M. J.; Nieminen, T.; Olenius, T.; Onnela, A.; Petaja, T.; Riccobono, F.; Riipinen, I.; Rissanen, M.; Rondo, L.; Ruuskanen, T.; Santos, F. D.; Sarnela, N.; Schallhart, S.; Schnitzhofer, R.; Seinfeld, J. H.; Simon, M.; Sipila, M.; Stozhkov, Y.; Stratmann, F.; Tome, A.; Trostl, J.; Tsagkogeorgas, G.; Vaattovaara, P.; Viisanen, Y.; Virtanen, A.; Vrtala, A.; Wagner, P. E.; Weingartner, E.; Wex, H.; Williamson, C.;

DOI: 10.1021/acs.est.7b02294
Environ. Sci. Technol. 2017, 51, 8422−8431

Wimmer, D.; Ye, P.; Yli-Juuti, T.; Carslaw, K. S.; Kulmala, M.; Curtius, J.; Baltensperger, U.; Worsnop, D. R.; Vehkamaki, H.; Kirkby, J. Molecular Understanding of Sulphuric Scid-amine Particle Nucleation in the Atmosphere. *Nature* **2013**, *502* (7471), 359−363.
(26) Ehn, M.; Thornton, J. A.; Kleist, E.; Sipila, M.; Junninen, H.; Pullinen, I.; Springer, M.; Rubach, F.; Tillmann, R.; Lee, B.; Lopez-Hilfiker, F.; Andres, S.; Acir, I.-H.; Rissanen, M.; Jokinen, T.; Schobesberger, S.; Kangasluoma, J.; Kontkanen, J.; Nieminen, T.; Kurten, T.; Nielsen, L. B.; Jorgensen, S.; Kjaergaard, H. G.; Canagaratna, M.; Maso, M. D.; Berndt, T.; Petaja, T.; Wahner, A.; Kerminen, V.-M.; Kulmala, M.; Worsnop, D. R.; Wildt, J.; Mentel, T. F. A Large Source of Low-volatility Secondary Organic Aerosol. *Nature* **2014**, *506* (7489), 476−479.
(27) Wang, Y. H.; Liu, Z. R.; Zhang, J. K.; Hu, B.; Ji, D. S.; Yu, Y. C.; Wang, Y. S. Aerosol Physicochemical Properties and Implications for Visibility During an Intense Haze Episode During Winter in Beijing. *Atmos. Chem. Phys.* **2015**, *15* (6), 3205−3215.
(28) Kirkby, J.; Curtius, J.; Almeida, J.; Dunne, E.; Duplissy, J.; Ehrhart, S.; Franchin, A.; Gagne, S.; Ickes, L.; Kurten, A.; Kupc, A.; Metzger, A.; Riccobono, F.; Rondo, L.; Schobesberger, S.; Tsagkogeorgas, G.; Wimmer, D.; Amorim, A.; Bianchi, F.; Breitenlechner, M.; David, A.; Dommen, J.; Downard, A.; Ehn, M.; Flagan, R. C.; Haider, S.; Hansel, A.; Hauser, D.; Jud, W.; Junninen, H.; Kreissl, F.; Kvashin, A.; Laaksonen, A.; Lehtipalo, K.; Lima, J.; Lovejoy, E. R.; Makhmutov, V.; Mathot, S.; Mikkila, J.; Minginette, P.; Mogo, S.; Nieminen, T.; Onnela, A.; Pereira, P.; Petaja, T.; Schnitzhofer, R.; Seinfeld, J. H.; Sipila, M.; Stozhkov, Y.; Stratmann, F.; Tome, A.; Vanhanen, J.; Viisanen, Y.; Vrtala, A.; Wagner, P. E.; Walther, H.; Weingartner, E.; Wex, H.; Winkler, P. M.; Carslaw, K. S.; Worsnop, D. R.; Baltensperger, U.; Kulmala, M. Role of Sulphuric Acid, Ammonia and Galactic Cosmic Rays in Atmospheric Aerosol Nucleation. *Nature* **2011**, *476* (7361), 429−433.
(29) Kurtén, T.; Loukonen, V.; Vehkamäki, H.; Kulmala, M. Amines Are Likely to Enhance Neutral and Ion-induced Sulfuric Acid-water Nucleation in the Atmosphere more Effectively than Ammonia. *Atmos. Chem. Phys.* **2008**, *8* (14), 4095−4103.
(30) Loukonen, V.; Kurtén, T.; Ortega, I. K.; Vehkamäki, H.; Pádua, A. A. H.; Sellegri, K.; Kulmala, M. Enhancing Effect of Dimethylamine in Sulfuric Acid Nucleation in the Presence of Water − a Computational Study. *Atmos. Chem. Phys.* **2010**, *10* (10), 4961−4974.
(31) Murphy, S. M.; Sorooshian, A.; Kroll, J. H.; Ng, N. L.; Chhabra, P.; Tong, C.; Surratt, J. D.; Knipping, E.; Flagan, R. C.; Seinfeld, J. H. Secondary Aerosol Formation from Atmospheric Reactions of Aliphatic Amines. *Atmos. Chem. Phys.* **2007**, *7* (9), 2313−2337.
(32) Berndt, T.; Stratmann, F.; Sipilä, M.; Vanhanen, J.; Petäjä, T.; Mikkilä, J.; Grüner, A.; Spindler, G.; Lee Mauldin Iii, R.; Curtius, J.; Kulmala, M.; Heintzenberg, J. Laboratory Study on New Particle Formation from the Reaction OH + SO_2: Influence of Experimental Conditions, H_2O Vapour, NH_3 and the Amine Tert-butylamine on the Overall Process. *Atmos. Chem. Phys.* **2010**, *10* (15), 7101−7116.
(33) Smith, J. N.; Barsanti, K. C.; Friedli, H. R.; Ehn, M.; Kulmala, M.; Collins, D. R.; Scheckman, J. H.; Williams, B. J.; McMurry, P. H. Observations of Aminium Salts in Atmospheric Nanoparticles and Possible Climatic Implications. *Proc. Natl. Acad. Sci. U. S. A.* **2010**, *107* (15), 6634−6639.
(34) Zhao, J.; Smith, J. N.; Eisele, F. L.; Chen, M.; Kuang, C.; McMurry, P. H. Observation of Neutral Sulfuric Acid-amine Containing Clusters in Laboratory and Ambient Measurements. *Atmos. Chem. Phys.* **2011**, *11* (21), 10823−10836.
(35) Erupe, M. E.; Viggiano, A. A.; Lee, S. H. The Effect of Trimethylamine on Atmospheric Nucleation Involving H_2SO_4. *Atmos. Chem. Phys.* **2011**, *11* (10), 4767−4775.
(36) Lehtipalo, K.; Rondo, L.; Kontkanen, J.; Schobesberger, S.; Jokinen, T.; Sarnela, N.; Kürten, A.; Ehrhart, S.; Franchin, A.; Nieminen, T.; Riccobono, F.; Sipilä, M.; Yli-Juuti, T.; Duplissy, J.; Adamov, A.; Ahlm, L.; Almeida, J.; Amorim, A.; Bianchi, F.; Breitenlechner, M.; Dommen, J.; Downard, A. J.; Dunne, E. M.; Flagan, R. C.; Guida, R.; Hakala, J.; Hansel, A.; Jud, W.; Kangasluoma, J.; Kerminen, V.-M.; Keskinen, H.; Kim, J.; Kirkby, J.; Kupc, A.; Kupiainen-Määttä, O.; Laaksonen, A.; Lawler, M. J.; Leiminger, M.; Mathot, S.; Olenius, T.; Ortega, I. K.; Onnela, A.; Petäjä, T.; Praplan, A.; Rissanen, M. P.; Ruuskanen, T.; Santos, F. D.; Schallhart, S.; Schnitzhofer, R.; Simon, M.; Smith, J. N.; Tröstl, J.; Tsagkogeorgas, G.; Tomé, A.; Vaattovaara, P.; Vehkamäki, H.; Vrtala, A. E.; Wagner, P. E.; Williamson, C.; Wimmer, D.; Winkler, P. M.; Virtanen, A.; Donahue, N. M.; Carslaw, K. S.; Baltensperger, U.; Riipinen, I.; Curtius, J.; Worsnop, D. R.; Kulmala, M. The Effect of Acid−base Clustering and Ions on the Growth of Atmospheric Nano-particles. *Nat. Commun.* **2016**, *7*, 11594.
(37) Chen, M.; Titcombe, M.; Jiang, J.; Jen, C.; Kuang, C.; Fischer, M. L.; Eisele, F. L.; Siepmann, J. I.; Hanson, D. R.; Zhao, J.; McMurry, P. H. Acid−base Chemical Reaction Model for Nucleation Rates in the Polluted Atmospheric Boundary Layer. *Proc. Natl. Acad. Sci. U. S. A.* **2012**, *109* (46), 18713−18718.
(38) Xu, Z.-Z.; Fan, H.-J. Competition Between H_2SO_4-$(CH_3)_3N$ and H_2SO_4−H_2O Interactions: Theoretical Studies on the Clusters $[(CH_3)_3N]\cdot(H_2SO_4)\cdot(H_2O)_{3-7}$. *J. Phys. Chem. A* **2015**, *119* (34), 9160−9166.
(39) Lv, S.-S.; Miao, S.-K.; Ma, Y.; Zhang, M.-M.; Wen, Y.; Wang, C.-Y.; Zhu, Y.-P.; Huang, W. Properties and Atmospheric Implication of Methylamine−Sulfuric Acid−Water Clusters. *J. Phys. Chem. A* **2015**, *119* (32), 8657−8666.
(40) Nadykto, A.; Yu, F.; Jakovleva, M.; Herb, J.; Xu, Y. Amines in the Earth's Atmosphere: A Density Functional Theory Study of the Thermochemistry of Pre-Nucleation Clusters. *Entropy* **2011**, *13* (2), 554−569.
(41) Nadykto, A.; Herb, J.; Yu, F.; Xu, Y.; Nazarenko, E. Estimating the Lower Limit of the Impact of Amines on Nucleation in the Earth's Atmosphere. *Entropy* **2015**, *17* (5), 2764−2780.
(42) Nadykto, A. B.; Herb, J.; Yu, F.; Xu, Y. Enhancement in the Production of Nucleating Clusters due to Dimethylamine and Large Uncertainties in the Thermochemistry of Amine-enhanced Nucleation. *Chem. Phys. Lett.* **2014**, *609*, 42−49.
(43) Jen, C. N.; McMurry, P. H.; Hanson, D. R. Stabilization of Sulfuric Acid Dimers by Ammonia, Methylamine, Dimethylamine, and Trimethylamine. *J. Geophys. Res. Atmos.* **2014**, *119* (12), 7502−7514.
(44) Jen, C. N.; Bachman, R.; Zhao, J.; McMurry, P. H.; Hanson, D. R. Diamine-sulfuric Acid Reactions Are a Potent Source of New Particle Formation. *Geophys. Res. Lett.* **2016**, *43* (2), 867−873.
(45) Elm, J.; Jen, C. N.; Kurtén, T.; Vehkamäki, H. Strong Hydrogen Bonded Molecular Interactions between Atmospheric Diamines and Sulfuric Acid. *J. Phys. Chem. A* **2016**, *120* (20), 3693−3700.
(46) Hall, H. K. Correlation of the Base Strengths of Amines1. *J. Am. Chem. Soc.* **1957**, *79* (20), 5441−5444.
(47) McGrath, M. J.; Olenius, T.; Ortega, I. K.; Loukonen, V.; Paasonen, P.; Kurtén, T.; Kulmala, M.; Vehkamäki, H. Atmospheric Cluster Dynamics Code: a flexible method for solution of the birth-death equations. *Atmos. Chem. Phys.* **2012**, *12* (5), 2345−2355.
(48) Olenius, T.; Kupiainen-Maatta, O. I.; Kurtén, T.; Vehkamäki, H.; Ortega, I. K. Free Energy Barrier in the Growth of Sulfuric Acid−ammonia and Sulfuric Acid−dimethylamine Clusters. *J. Chem. Phys.* **2013**, *139* (8), 084312.
(49) Ortega, I. K.; Kupiainen, O.; Kurtén, T.; Olenius, T.; Wilkman, O.; McGrath, M. J.; Loukonen, V.; Vehkamäki, H. From Quantum Chemical Formation Free Energies to Evaporation Rates. *Atmos. Chem. Phys.* **2012**, *12* (1), 225−235.
(50) Elm, J.; Fard, M.; Bilde, M.; Mikkelsen, K. V. Interaction of Glycine with Common Atmospheric Nucleation Precursors. *J. Phys. Chem. A* **2013**, *117* (48), 12990−12997.
(51) Elm, J.; Myllys, N.; Hyttinen, N.; Kurtén, T. Computational Study of the Clustering of a Cyclohexene Autoxidation Product $C_6H_8O_7$ with Itself and Sulfuric Acid. *J. Phys. Chem. A* **2015**, *119* (30), 8414−8421.
(52) Frisch, M. J.; Trucks, G. W.; Schlegel, H.B.; Scuseria, G. E.; Robb, M. A.; Cheeseman, J. R., et al. *Gaussian 09*; 2009.
(53) Elm, J.; Bilde, M.; Mikkelsen, K. V. Assessment of Binding Energies of Atmospherically Relevant Clusters. *Phys. Chem. Chem. Phys.* **2013**, *15* (39), 16442−16445.

DOI: 10.1021/acs.est.7b02294
Environ. Sci. Technol. 2017, 51, 8422−8431

(54) Elm, J.; Kristensen, K. Basis Set Convergence of the Binding Eenergies of Strongly Hydrogen-bonded Atmospheric Clusters. *Phys. Chem. Chem. Phys.* **2017**, *19* (2), 1122−1133.
(55) Riplinger, C.; Neese, F. An Efficient and Near Linear Scaling Pair Natural Orbital Based Local Coupled Cluster Method. *J. Chem. Phys.* **2013**, *138* (3), 034106.
(56) Riplinger, C.; Sandhoefer, B.; Hansen, A.; Neese, F. Natural Triple Excitations in Local Coupled Cluster Calculations with Pair Natural Orbitals. *J. Chem. Phys.* **2013**, *139* (13), 134101.
(57) Neese, F. The ORCA program system. *Wiley Interdiscip. Rev. Comput. Mol. Sci.* **2012**, *2* (1), 73−78.
(58) Myllys, N.; Elm, J.; Halonen, R.; Kurtén, T.; Vehkamäki, H. Coupled Cluster Evaluation of the Stability of Atmospheric Acid−Base Clusters with up to 10 Molecules. *J. Phys. Chem. A* **2016**, *120* (4), 621−630.
(59) Vorobyov, I.; Yappert, M. C.; DuPré, D. B. Hydrogen Bonding in Monomers and Dimers of 2-Aminoethanol. *J. Phys. Chem. A* **2002**, *106* (4), 668−679.
(60) Olenius, T.; Kurtén, T.; Henschel, H.; Kupiainen-Määttä, O.; Ortega, I. K.; Vehkamäki, H.; Riipinen, I.; Halonen, R.; Jen, C. New Particle Formation from Sulfuric Acid and Amines: Comparison of Mono-, Di-, and Trimethylamines. *J. Geophys. Res.: Atmos.* **2017**, DOI: 10.1002/2017JD026501.
(61) Henschel, H.; Kurtén, T.; Vehkamäki, H. Computational Study on the Effect of Hydration on New Particle Formation in the Sulfuric Acid/Ammonia and Sulfuric Acid/Dimethylamine Systems. *J. Phys. Chem. A* **2016**, *120* (11), 1886−1896.
(62) Kerminen, V. M.; Petäjä, T.; Manninen, H. E.; Paasonen, P.; Nieminen, T.; Sipilä, M.; Junninen, H.; Ehn, M.; Gagné, S.; Laakso, L.; Riipinen, I.; Vehkamäki, H.; Kurten, T.; Ortega, I. K.; Dal Maso, M.; Brus, D.; Hyvärinen, A.; Lihavainen, H.; Leppä, J.; Lehtinen, K. E. J.; Mirme, A.; Mirme, S.; Hõrrak, U.; Berndt, T.; Stratmann, F.; Birmili, W.; Wiedensohler, A.; Metzger, A.; Dommen, J.; Baltensperger, U.; Kiendler-Scharr, A.; Mentel, T. F.; Wildt, J.; Winkler, P. M.; Wagner, P. E.; Petzold, A.; Minikin, A.; Plass-Dülmer, C.; Pöschl, U.; Laaksonen, A.; Kulmala, M. Atmospheric Nucleation: Highlights of the EUCAARI Project and Future Directions. *Atmos. Chem. Phys.* **2010**, *10* (22), 10829−10848.
(63) Chen, H.; Varner, M. E.; Gerber, R. B.; Finlayson-Pitts, B. J. Reactions of Methanesulfonic Acid with Amines and Ammonia as a Source of New Particles in Air. *J. Phys. Chem. B* **2016**, *120* (8), 1526−1536.
(64) Ling, J.; Ding, X.; Li, Z.; Yang, J. First-Principles Study of Molecular Clusters Formed by Nitric Acid and Ammonia. *J. Phys. Chem. A* **2017**, *121* (3), 661−668.
(65) DePalma, J. W.; Wang, J.; Wexler, A. S.; Johnston, M. V. Growth of Ammonium Bisulfate Clusters by Adsorption of Oxygenated Organic Molecules. *J. Phys. Chem. A* **2015**, *119* (45), 11191−11198.
(66) DePalma, J. W.; Doren, D. J.; Johnston, M. V. Formation and Growth of Molecular Clusters Containing Sulfuric Acid, Water, Ammonia, and Dimethylamine. *J. Phys. Chem. A* **2014**, *118* (29), 5464−5473.
(67) Ge, X.; Wexler, A. S.; Clegg, S. L. Atmospheric Amines − Part I. A review. *Atmos. Environ.* **2011**, *45* (3), 524−546.
(68) Price, D. J.; Clark, C. H.; Tang, X.; Cocker, D. R.; Purvis-Roberts, K. L.; Silva, P. J. Proposed Chemical Mechanisms leading to Secondary Organic Aerosol in the Reactions of Aliphatic Amines with Hydroxyl and Nitrate Radicals. *Atmos. Environ.* **2014**, *96*, 135−144.
(69) Angelino, S.; Suess, D. T.; Prather, K. A. Formation of Aerosol Particles from Reactions of Secondary and Tertiary Alkylamines: Characterization by Aerosol Time-of-Flight Mass Spectrometry. *Environ. Sci. Technol.* **2001**, *35* (15), 3130−3138.
(70) Zheng, J.; Hu, M.; Zhang, R.; Yue, D.; Wang, Z.; Guo, S.; Li, X.; Bohn, B.; Shao, M.; He, L.; Huang, X.; Wiedensohler, A.; Zhu, T. Measurements of Gaseous H_2SO_4 by AP-ID-CIMS During CARE-Beijing 2008 Campaign. *Atmos. Chem. Phys.* **2011**, *11* (15), 7755−7765.
(71) Berresheim, H.; Elste, T.; Tremmel, H. G.; Allen, A. G.; Hansson, H. C.; Rosman, K.; Dal Maso, M.; Mäkelä, J. M.; Kulmala, M.; O'Dowd, C. D. Gas-aerosol relationships of H_2SO_4, MSA, and OH: Observations in the Coastal Marine Boundary Layer at Mace Head, Ireland. *J. Geophys. Res.* **2002**, *107* (D19), 5-1−5-12.
(72) Jokinen, T.; Sipilä, M.; Junninen, H.; Ehn, M.; Lönn, G.; Hakala, J.; Petäjä, T.; Mauldin, R. L.; Kulmala, M.; Worsnop, D. R. Atmospheric Sulphuric Acid and Neutral Cluster Mmeasurements Using CI-APi-TOF. *Atmos. Chem. Phys.* **2012**, *12* (9), 4117−4125.

DOI: 10.1021/acs.est.7b02294
Environ. Sci. Technol. 2017, 51, 8422−8431